Supplementary Material

Long-term mercury isotope evidence for a shift toward background-dominated urban atmospheric mercury in North China under sustained emission controls

Chao Zhang[1], Xiaomiao Mu[1], Ruoyu Sun[1], Songjing Li[1], Zhao Wang[1], Xinguang Li[1], Muhammad Asif Sherliyat[1], Xiaojian Wang[1], Yi Liu[1], Wang Zheng[1], and Jiubin Chen[1]

[1]Institute of Surface-Earth System Science, School of Earth System Science, Tianjin University, Tianjin 300072, China

Correspondence to: Ruoyu Sun (ruoyu.sun@tju.edu.cn)

Text S1. Mercury blanks of carbon adsorbents

The intrinsic blank values for the adsorbents were 0.40 ± 0.49 ng/g for chlorinated activated carbon (n = 12) and 0.09 ± 0.11 ng/g for sulfur-impregnated activated carbon (n = 2). The amount of chlorinated activated carbon used in the active sampling system was 0.40 ± 0.04 g (n = 66), corresponding to an average blank Hg mass of ~ 0.16 ng. This represented an average of 1.67% (0.29–4.30%, n = 66) of the total Hg collected in the samples. For MerPAS sampling, sulfur-impregnated activated carbon masses averaged 0.57 ± 0.04 g (n = 36), yielding an average blank Hg mass of ~ 0.05 ng. Additional blanks were analyzed to assess potential contamination introduced during sampler storage, transportation, and handling. MerPAS units were stored and transported in sealed, double-bagged packaging, resulting in measured blank concentrations of 0.05 ± 0.01 ng/g (n = 2). MerPAS samplers were opened at the sampling site and exposed to ambient air for 10 s before resealing, resulting in an average field blank concentration of 0.58 ± 0.14 ng/g (n = 10). This accounted for 3.57% (2.89–4.56%, n = 10) of the total Hg mass in collected samples, indicating that blank contributions were minor.

Text S2. Total Hg concentration measurement

Total Hg concentrations in samples, including chlorinated activated and sulfur-impregnated activated carbon, were directly measured using the DMA-80 evo. This instrument operates by thermally decomposing the sample, selectively trapping volatilized Hg(0) vapor on a gold amalgamator, followed by thermal desorption and detection of Hg(0) vapor via atomic absorption spectrophotometry at 253.7 nm (EPA-7473). Hg concentrations in the trapping solutions obtained after sample processing were quantified using a Tekran 2600 cold vapor atomic fluorescence spectrometer (CV-AFS) (EPA-1631E). Analytical uncertainty was assessed using GBW 07311 (sediment; 72 ± 14 ng g^{-1}) for DMA-80, and NIST 3133 and NIST 8610 Hg standard solutions for Tekran 2600. The combined analytical uncertainty of total Hg concentrations in standards was within ± 8% of their certified values. Replicate sample analyses ($n \geq 2$) exhibited relative standard deviations < 5%.

Text S3. Preconcentration of Hg for isotope analysis

Based on the measured Hg concentrations in chlorinated activated carbon and sulfur-impregnated activated carbon samples, 0.2-0.4 g of each sample was preconcentrated for Hg using a modified DMA method (Sun et al., 2023, 2025). This was achieved via a drying/decomposition-catalyst system of the DMA-80 evo. Briefly, weighed samples were loaded into nickel boats and introduced into the drying/decomposition furnace, where all Hg species were thermally released as Hg^0 vapor through programmed heating stages. During thermal decomposition, a continuous flow of oxygen (250 mL/min) carried the decomposition products through a heated catalyst bed, which efficiently removed halogens and nitrogen- and sulfur-containing gases from the sample matrix. The released Hg(0) vapor was subsequently directed into an impinger containing an oxidizing trapping solution with 40% HNO_3:HCl (2:1, v/v) and 1% (v/v) BrCl. To prolong the lifetime of the DMA catalyst and reduce matrix interference, ~0.1 g of sodium carbonate (pre-baked at 450 °C to remove residual Hg) was added to the boats containing sulfur-impregnated activated carbon, following Szponar et al. (2020). Procedural blanks and CRMs were processed alongside the samples following identical procedures. The average Hg preconcentration recoveries were 95-99% for procedural CRMs (Table S1) and 96 ± 4% for samples (Tables S4-S7), which were calculated by comparing Hg masses before and after Hg preconcentration.

Table S1. Summary of Hg isotope compositions and uncertainties of secondary Hg standard solutions and procedural certified reference materials (CRMs).

Standard	n	Recoveries (%)	δ^{202}Hg (‰)	2SD (‰)	Δ^{199}Hg (‰)	2SD (‰)	Δ^{200}Hg (‰)	2SD (‰)	Δ^{201}Hg (‰)	2SD (‰)	Δ^{204}Hg (‰)	2SD (‰)
NIST RM 8610	40	-	-0.55	0.06	-0.02	0.04	0.01	0.03	-0.03	0.05	-0.01	0.06
GBW 07310	9	95.26%	-0.60	0.06	-0.27	0.06	-0.01	0.04	-0.24	0.05	0.03	0.04
GBW 07405	10	98.79%	-1.63	0.08	-0.36	0.06	0.00	0.05	-0.34	0.04	0.04	0.07
GBW 07310*	12	-	-0.52	0.15	-0.26	0.10	0.00	0.05	-0.22	0.10	0.00	0.06
GBW 07405**	4	111%	-1.77	0.09	-0.33	0.03	0.00	0.02	-0.31	0.06	0.00	0.05

Note: * data cited from Sun et al., 2023; ** data cited from Sun et al., 2025.

Table S2. Atmospheric GEM concentrations derived from passive air samplers in the urban Nankai site, Tianjin.

ID	Sampling date	Sampling durations (days)	Average Temperature (°C)	Average wind speed (m/s)	sampling rate (m^3/day)		GEM (ng/m^3)
PAS-1-1	2021/10/21-11/29	40	8.1	2.2	0.145		2.11 2.09
						average	**2.10**
PAS-1-2	2022/03/31-05/20	51	17.5	3.1	0.155		1.24 1.26
						average	**1.25**
PAS-1-3	20220525-0716	53	26.5	2.7	0.166		1.45 1.52
						average	**1.48**
PAS-1-4	20220905-1022	48	18.9	2.6	0.156		1.11 1.13
						average	**1.12**
PAS-2-1	20240201-0301	29	0.4	2.4	0.137		1.19 1.20
						average	**1.20**
PAS-2-2	20240301-0401	31	9.3	3.0	0.147		1.03 1.04
						average	**1.04**
PAS-2-3	20240401-0515	44	16.8	2.9	0.155		0.94 0.94
						average	**0.94**
PAS-2-4	20240515-0701	47	27.8	2.6	0.167		1.41 1.40
						average	**1.41**

							1.64
PAS-2-5	20240701-0815	45	27.5	2.4	0.167		1.58
						average	**1.61**
							1.56
PAS-2-6	20240815-0924	40	22.0	2.0	0.160		1.59
						average	**1.58**
							1.43
PAS-2-7	20240924-1114	51	11.2	2.0	0.148		1.43
						average	**1.43**
							1.68
PAS-2-8	20241114-0109	56	-0.9	2.4	0.136		1.72
						average	**1.70**

Table S3. Atmospheric GEM concentrations derived from passive air samplers deployed for short-term inter-city comparisons.

Sample ID	Location	Sampling date	Sample durations (days)	Average temperature (°C)	Average wind speed (m/s)	sampling rate (m^3/day)		GEM (ng/m^3)
PAS-Nankai	Nankai, Tianjin, China	20250109-0303	53	-0.7	2.6	0.136		1.86
								1.77
							average	**1.81**
PAS-Binhai	Binhai, Tianjin, China	20250109-0303	53	1.0	4.7	0.137		1.65
								1.57
							average	**1.61**
PAS-Tangshan	Tangshan, Hebei Province, China	20250128-0309	40	0.2	3.1	0.141		1.76
								1.86
							average	**1.81**
PAS-Chengde	Chengde, Hebei Province, China	20250124-0224	31	-10.5	4.0	0.134		1.46
								1.53
							average	**1.49**
PAS-Jingzhou	Jingzhou, Hubei Province, China	20250121-0221	31	19.5	3.4	0.145		1.50
								1.63
							average	**1.56**
PAS-Karachi	Karachi, Sindh Province, Pakistan	20250124-0312	48	20.0	4.0	0.159		5.81
								6.03
							average	**5.92**

Table S4. Atmospheric GEM isotopic compositions derived from passive air samplers.

Sample ID		Recoveries (%)	δ^{202}Hg (‰)	2SD (‰)	Δ^{199}Hg (‰)	2SD (‰)	Δ^{200}Hg (‰)	2SD (‰)	Δ^{201}Hg (‰)	2SD (‰)	Δ^{204}Hg (‰)	2SD (‰)
		94.56	0.14	0.08	-0.11	0.06	-0.03	0.05	-0.13	0.04	0.09	0.07
PAS-1-1		100.87	0.14	0.08	-0.15	0.06	0.00	0.05	-0.15	0.04	0.09	0.07
	average	**97.71**	**0.14**	**0.08**	**-0.13**	**0.06**	**-0.01**	**0.05**	**-0.14**	**0.04**	**0.09**	**0.07**
		95.97	0.02	0.08	-0.16	0.06	-0.03	0.05	-0.12	0.04	0.06	0.07
PAS-1-2		91.79	0.03	0.08	-0.15	0.06	-0.04	0.05	-0.14	0.04	0.09	0.07
	average	**93.88**	**0.02**	**0.08**	**-0.15**	**0.06**	**-0.03**	**0.05**	**-0.13**	**0.04**	**0.07**	**0.07**
		99.15	0.02	0.08	-0.18	0.06	-0.03	0.05	-0.17	0.04	0.07	0.07
PAS-1-3		94.08	0.02	0.08	-0.18	0.06	-0.04	0.05	-0.12	0.04	0.05	0.07
	average	**96.62**	**0.02**	**0.08**	**-0.18**	**0.06**	**-0.03**	**0.05**	**-0.15**	**0.04**	**0.06**	**0.07**
		92.02	0.26	0.08	-0.15	0.06	-0.03	0.05	-0.15	0.04	0.04	0.07
PAS-1-4		99.67	0.18	0.08	-0.17	0.06	-0.03	0.05	-0.16	0.04	0.05	0.07
	average	**95.85**	**0.22**	**0.08**	**-0.16**	**0.06**	**-0.03**	**0.05**	**-0.15**	**0.04**	**0.05**	**0.07**
		102.29	-0.02	0.08	-0.15	0.06	-0.01	0.05	-0.16	0.04	0.09	0.07
PAS-2-1		90.93	-0.01	0.08	-0.15	0.06	-0.01	0.05	-0.16	0.04	0.08	0.07
	average	**96.61**	**-0.01**	**0.08**	**-0.15**	**0.06**	**-0.01**	**0.05**	**-0.16**	**0.04**	**0.09**	**0.07**
		96.08	0.46	0.08	-0.18	0.06	-0.01	0.05	-0.20	0.04	0.10	0.07
PAS-2-2		93.82	0.40	0.08	-0.15	0.06	-0.04	0.05	-0.19	0.04	0.08	0.07
	average	**94.95**	**0.43**	**0.08**	**-0.16**	**0.06**	**-0.02**	**0.05**	**-0.19**	**0.04**	**0.09**	**0.07**
		101.05	0.20	0.08	-0.21	0.06	-0.08	0.05	-0.18	0.04	0.04	0.07
PAS-2-3		93.21	0.05	0.08	-0.15	0.06	-0.06	0.05	-0.21	0.04	0.06	0.07
	average	**97.13**	**0.13**	**0.08**	**-0.18**	**0.06**	**-0.07**	**0.05**	**-0.19**	**0.04**	**0.05**	**0.07**
		92.79	-0.11	0.08	-0.16	0.06	-0.05	0.05	-0.16	0.04	0.07	0.07
PAS-2-4		96.37	0.02	0.08	-0.16	0.06	-0.03	0.05	-0.19	0.04	0.10	0.07
	average	**94.58**	**-0.04**	**0.08**	**-0.16**	**0.06**	**-0.04**	**0.05**	**-0.17**	**0.04**	**0.08**	**0.07**
PAS-2-5		96.50	0.08	0.08	-0.15	0.06	-0.03	0.05	-0.15	0.04	0.13	0.07

		95.86	0.18	0.08	-0.11	0.06	-0.01	0.05	-0.16	0.04	0.08	0.07
	average	**96.18**	**0.13**	**0.08**	**-0.13**	**0.06**	**-0.02**	**0.05**	**-0.16**	**0.04**	**0.11**	**0.07**
		94.16	-0.03	0.08	-0.16	0.06	-0.08	0.05	-0.18	0.04	0.02	0.07
PAS-2-6		94.40	0.12	0.08	-0.09	0.06	0.01	0.05	-0.12	0.04	0.05	0.07
	average	**94.28**	**0.04**	**0.08**	**-0.13**	**0.06**	**-0.04**	**0.05**	**-0.15**	**0.04**	**0.03**	**0.07**
		98.94	-0.14	0.08	-0.18	0.06	-0.02	0.05	-0.17	0.04	-0.01	0.07
PAS-2-7		104.48	-0.19	0.08	-0.20	0.06	-0.04	0.05	-0.22	0.04	0.05	0.07
	average	**101.71**	**-0.17**	**0.08**	**-0.19**	**0.06**	**-0.03**	**0.05**	**-0.20**	**0.04**	**0.02**	**0.07**
		99.33	0.10	0.08	-0.22	0.06	-0.06	0.05	-0.22	0.04	0.07	0.07
PAS-2-8		109.09	-0.03	0.08	-0.26	0.06	-0.04	0.05	-0.23	0.04	0.02	0.07
	average	**104.21**	**0.03**	**0.08**	**-0.24**	**0.06**	**-0.05**	**0.05**	**-0.23**	**0.04**	**0.05**	**0.07**
		96.35	0.00	0.08	-0.23	0.06	-0.10	0.05	-0.22	0.04	-0.05	0.07
PAS-Nankai		100.27	0.04	0.08	-0.18	0.06	-0.08	0.05	-0.25	0.04	-0.06	0.07
	average	**98.31**	**0.02**	**0.08**	**-0.21**	**0.06**	**-0.09**	**0.05**	**-0.24**	**0.04**	**-0.05**	**0.07**
		93.42	0.06	0.08	-0.24	0.06	-0.04	0.05	-0.24	0.04	0.06	0.07
PAS-Binhai		98.50	0.10	0.08	-0.27	0.06	-0.08	0.05	-0.27	0.04	0.04	0.07
	average	**95.96**	**0.08**	**0.08**	**-0.26**	**0.06**	**-0.06**	**0.05**	**-0.25**	**0.04**	**0.05**	**0.07**
		94.74	0.09	0.08	-0.20	0.06	-0.04	0.05	-0.22	0.04	0.03	0.07
PAS-Tangshan		91.90	0.13	0.08	-0.24	0.06	-0.05	0.05	-0.20	0.04	0.07	0.07
	average	**93.32**	**0.11**	**0.08**	**-0.22**	**0.06**	**-0.05**	**0.05**	**-0.21**	**0.04**	**0.05**	**0.07**
		94.68	0.47	0.08	-0.24	0.06	-0.07	0.05	-0.20	0.04	0.13	0.07
PAS-Chengde		91.76	0.49	0.08	-0.22	0.06	-0.05	0.05	-0.16	0.04	0.13	0.07
	average	**93.22**	**0.48**	**0.08**	**-0.23**	**0.06**	**-0.06**	**0.05**	**-0.18**	**0.04**	**0.13**	**0.07**
		92.94	0.35	0.08	-0.23	0.06	-0.04	0.05	-0.20	0.04	0.09	0.07
PAS-Jingzhou		91.76	0.35	0.08	-0.17	0.06	-0.02	0.05	-0.18	0.04	0.11	0.07
	average	**92.35**	**0.35**	**0.08**	**-0.20**	**0.06**	**-0.03**	**0.05**	**-0.19**	**0.04**	**0.10**	**0.07**
		91.70	-0.65	0.08	-0.01	0.06	0.01	0.05	-0.06	0.04	0.04	0.07
PAS-Karachi		94.24	-0.55	0.08	-0.08	0.06	-0.03	0.05	-0.06	0.04	0.04	0.07
	average	**92.97**	**-0.60**	**0.08**	**-0.04**	**0.06**	**-0.01**	**0.05**	**-0.06**	**0.04**	**0.04**	**0.07**

Note: All $\delta^{202}Hg$ values were reported as post-correction values.

Table S5. Atmospheric GEM concentrations and isotopic compositions derived from active pump-trap sampling during Phase I (2018) and Phase II (2021-2022) in the urban Nankai site, Tianjin.

Sample ID	Date	Recoveries (%)	GEM (ng/m^3)	δ^{202}Hg (‰)	2SD (‰)	Δ^{199}Hg (‰)	2SD (‰)	Δ^{200}Hg (‰)	2SD (‰)	Δ^{201}Hg (‰)	2SD (‰)	Δ^{204}Hg (‰)	2SD (‰)
Phase I: 2018													
1-01	20181106-1107	94.22	4.68	-0.78	0.08	-0.02	0.06	0.03	0.05	-0.05	0.04	0.02	0.07
1-02	20181107-1107	93.68	4.28	-1.03	0.08	-0.01	0.06	0.04	0.05	-0.04	0.04	-0.07	0.07
1-03	20181107-1108	95.30	4.83	-0.61	0.08	-0.08	0.06	-0.01	0.05	-0.07	0.04	0.01	0.07
Phase II: 2021–2022													
2-01	20211021-1022	96.85	0.49	1.14	0.08	–0.18	0.06	–0.02	0.05	-0.20	0.04	0.06	0.07
2-02	20211027-1028	94.11	1.49	0.01	0.08	–0.11	0.06	–0.04	0.05	-0.12	0.04	0.04	0.07
2-03	20211101-1103	95.63	1.96	–0.18	0.08	–0.15	0.06	–0.03	0.05	-0.15	0.04	0.05	0.07
2-04	20211104-1106	92.04	4.75	–0.49	0.08	–0.10	0.06	–0.01	0.05	-0.11	0.04	0.08	0.07
2-05	20211111-1113	104.69	0.99	0.64	0.08	–0.20	0.06	–0.05	0.05	-0.21	0.04	0.10	0.07
2-06	20211118-1120	99.52	1.85	0.06	0.08	–0.16	0.06	–0.03	0.05	-0.15	0.04	0.01	0.07
2-07	20211121-1123	100.20	0.91	1.38	0.08	–0.21	0.06	–0.07	0.05	-0.17	0.04	0.04	0.07
2-08	20211124-1126	107.03	2.58	–0.03	0.08	–0.22	0.06	–0.04	0.05	-0.19	0.04	0.07	0.07
2-09	20211128-1129	94.73	2.89	–0.12	0.08	–0.15	0.06	0.00	0.05	-0.17	0.04	0.05	0.07
2-10	20220331-0402	95.87	1.55	0.08	0.08	–0.15	0.06	–0.05	0.05	-0.17	0.04	0.01	0.07
2-11	20220403-0404	104.47	1.89	0.56	0.08	–0.15	0.06	–0.03	0.05	-0.12	0.04	0.00	0.07
2-12	20220407-0409	92.63	1.91	0.09	0.08	–0.08	0.06	–0.02	0.05	-0.08	0.04	0.01	0.07
2-13	20220417-0420	91.55	0.96	0.09	0.08	–0.11	0.06	–0.02	0.05	-0.10	0.04	0.06	0.07
2-14	20220422-0425	97.11	1.39	–0.11	0.08	–0.13	0.06	–0.01	0.05	-0.11	0.04	0.07	0.07
2-15	20220428-0501	91.23	1.05	0.41	0.08	–0.14	0.06	–0.02	0.05	-0.15	0.04	0.06	0.07
2-16	20220503-0506	93.12	0.65	0.55	0.08	–0.14	0.06	–0.04	0.05	-0.13	0.04	0.02	0.07
2-17	20220512-0515	93.13	0.81	0.44	0.08	–0.15	0.06	–0.04	0.05	-0.14	0.04	0.04	0.07
2-18	20220517-0520	94.37	0.95	–0.06	0.08	–0.07	0.06	–0.01	0.05	-0.09	0.04	0.03	0.07

2-19	20220525-0528	107.98	0.67	0.47	0.08	–0.17	0.06	–0.03	0.05	-0.16	0.04	0.01	0.07
2-20	20220530-0602	91.72	1.19	–0.10	0.08	–0.14	0.06	–0.05	0.05	-0.11	0.04	0.06	0.07
2-21	20220605-0608	97.62	0.80	0.30	0.08	–0.19	0.06	–0.04	0.05	-0.13	0.04	0.13	0.07
2-22	20220615-0618	97.96	2.01	–0.39	0.08	–0.10	0.06	–0.02	0.05	-0.12	0.04	0.04	0.07
2-23	20220619-0622	94.75	2.25	–0.34	0.08	–0.14	0.06	–0.03	0.05	-0.12	0.04	0.04	0.07
2-24	20220630-0703	92.75	1.59	–0.28	0.08	–0.11	0.06	–0.03	0.05	-0.12	0.04	0.06	0.07
2-25	20220713-0716	95.40	1.46	–0.06	0.08	–0.15	0.06	–0.02	0.05	-0.13	0.04	0.00	0.07
2-26	20220905-0907	103.21	0.55	0.28	0.08	–0.15	0.06	–0.05	0.05	-0.17	0.04	0.08	0.07
2-27	20220909-0912	90.41	1.03	–0.35	0.08	–0.15	0.06	–0.06	0.05	-0.16	0.04	0.04	0.07
2-28	20220918-0921	97.18	0.73	0.27	0.08	–0.20	0.06	–0.06	0.05	-0.17	0.04	0.06	0.07
2-29	20220924-0927	97.77	1.58	–0.24	0.08	–0.13	0.06	–0.01	0.05	-0.10	0.04	0.06	0.07
2-30	20221012-1015	98.89	1.41	–0.13	0.08	–0.13	0.06	–0.03	0.05	-0.12	0.04	0.02	0.07
2-31	20221019-1022	96.97	0.82	0.20	0.08	–0.18	0.06	–0.05	0.05	-0.15	0.04	0.11	0.07

Table S6. Atmospheric diurnal GEM concentrations and isotopic compositions derived from active pump-trap sampling during Phase III (2024-2025) in the urban Nankai site, Tianjin.

Sample ID	Start date	End date	Recoveries (%)	GEM (ng/m³)	δ^{202}Hg (‰)	2SD (‰)	Δ^{199}Hg (‰)	2SD (‰)	Δ^{200}Hg (‰)	2SD (‰)	Δ^{201}Hg (‰)	2SD (‰)	Δ^{204}Hg (‰)	2SD (‰)
Nankai-1-1	20241211/17:30	20241212/07:10	99.43	2.24	-0.06	0.08	-0.23	0.06	-0.04	0.05	-0.24	0.04	0.09	0.07
Nankai-1-2	20241212/07:15	20241212/5:30	96.49	2.48	-0.28	0.08	-0.22	0.06	-0.06	0.05	-0.26	0.04	0.03	0.07
Nankai-2-1	20241212/17:35	20241213/07:15	91.08	1.77	0.56	0.08	-0.20	0.06	-0.03	0.05	-0.13	0.04	0.08	0.07
Nankai-2-2	20241213/07:45	20241213/17:45	94.84	1.34	0.41	0.08	-0.10	0.06	-0.01	0.05	-0.12	0.04	0.09	0.07
Nankai-3-1	20241213/18:10	20241214/07:10	93.22	1.53	0.33	0.08	-0.22	0.06	-0.03	0.05	-0.16	0.04	0.19	0.07
Nankai-3-2	20241214/07:15	20241214/18:45	98.27	2.36	0.21	0.08	-0.14	0.06	-0.03	0.05	-0.13	0.04	0.13	0.07
Nankai-4-1	20241214/18:50	20241215/07:10	91.92	1.61	0.36	0.08	-0.13	0.06	-0.03	0.05	-0.13	0.04	0.16	0.07
Nankai-5-1	20250104/7:00	20250104/18:00	99.84	1.92	-0.36	0.08	-0.13	0.06	-0.01	0.05	-0.12	0.04	0.01	0.07
Nankai-5-2	20250104/18:00	20250105/7:00	98.03	2.55	-0.36	0.08	-0.19	0.06	-0.04	0.05	-0.17	0.04	0.04	0.07
Nankai-6-1	20250105/7:00	20250105/18:00	96.98	2.08	-0.27	0.08	-0.11	0.06	-0.02	0.05	-0.13	0.04	0.02	0.07
Nankai-6-2	20250105/18:00	20250106/7:00	94.05	1.54	0.02	0.08	-0.16	0.06	-0.04	0.05	-0.18	0.04	0.07	0.07
Nankai-7-1	20250106/7:00	20250106/18:00	101.01	1.31	0.14	0.08	-0.11	0.06	-0.03	0.05	-0.13	0.04	0.03	0.07
Nankai-7-2	20250106/18:00	20250107/7:00	94.03	1.23	-0.09	0.08	-0.18	0.06	-0.03	0.05	-0.13	0.04	0.14	0.07
Nankai-8-1	20250107/7:00	20250107/18:00	99.43	1.10	0.20	0.08	-0.21	0.06	-0.08	0.05	-0.16	0.04	0.05	0.07
Nankai-8-2	20250107/18:00	20250108/7:00	92.45	1.01	0.31	0.08	-0.16	0.06	-0.02	0.05	-0.17	0.04	0.07	0.07
Nankai-9-1	20250108/7:00	20250108/18:00	93.04	1.23	0.34	0.08	-0.11	0.06	-0.02	0.05	-0.16	0.04	0.10	0.07
Nankai-9-2	20250108/18:00	20250109/7:00	94.80	1.24	0.20	0.08	-0.23	0.06	-0.07	0.05	-0.16	0.04	0.20	0.07
Nankai-10-1	20250109/7:00	20250110/18:00	93.26	1.01	0.39	0.08	-0.21	0.06	-0.07	0.05	-0.16	0.04	0.11	0.07

Table S7. Atmospheric GEM concentrations and isotopic compositions derived from active pump-trap sampling during Phase III (2024-2025) in the suburban Binhai site, Tianjin

Sample ID	Start date	End date	Recoveries (%)	GEM (ng/m³)	δ^{202}Hg (‰)	2sd (‰)	Δ^{199}Hg (‰)	2sd (‰)	Δ^{200}Hg (‰)	2sd (‰)	Δ^{201}Hg (‰)	2sd (‰)	Δ^{204}Hg (‰)	2sd (‰)
Binhai-1	20241223/14:30	20241224/09:00	97.61	1.26	-0.02	0.08	-0.14	0.06	-0.04	0.05	-0.17	0.04	0.04	0.07
Binhai-2	20241225/09:00	20241226/09:00	95.46	1.66	0.23	0.08	-0.20	0.06	-0.04	0.05	-0.19	0.04	0.06	0.07
Binhai-3	20241226/09:00	20241227/09:00	94.58	1.15	0.38	0.08	-0.23	0.06	-0.07	0.05	-0.18	0.04	0.13	0.07
Binhai-4	20241227/09:00	20241228/09:00	94.22	1.40	0.41	0.08	-0.22	0.06	-0.04	0.05	-0.17	0.04	0.12	0.07
Binhai-5	20241228/09:00	20241229/09:00	93.23	1.15	0.19	0.08	-0.11	0.06	0.00	0.05	-0.16	0.04	0.04	0.07
Binhai-6	20241229/09:00	20241230/09:00	95.55	1.27	0.09	0.08	-0.18	0.06	-0.02	0.05	-0.20	0.04	0.08	0.07
Binhai-7	20241230/09:00	20241231/09:00	100.69	1.69	0.26	0.08	-0.16	0.06	-0.04	0.05	-0.19	0.04	0.13	0.07
Binhai-8	20241231/09:00	20250101/09:00	94.08	1.14	0.09	0.08	-0.12	0.06	-0.01	0.05	-0.12	0.04	0.05	0.07
Binhai-9	20250101/09:00	20250102/09:00	95.80	1.50	0.08	0.08	-0.21	0.06	-0.05	0.05	-0.14	0.04	-0.02	0.07
Binhai-10	20250102/09:00	20250103/09:00	98.63	1.47	0.28	0.08	-0.15	0.06	-0.04	0.05	-0.15	0.04	0.10	0.07

Table S8. Concentrations and isotopic compositions of GEM collected by passive samplers across different sites.

Site	Location (°)		n	GEM (ng/m^3)		δ^{202}Hg (‰)		Δ^{199}Hg (‰)		Δ^{200}Hg (‰)		Δ^{201}Hg (‰)		References
	longitude	Latitude		Mean	SD	Mean	uncertainty	Mean	uncertainty	Mean	uncertainty	Mean	uncertainty	
TJ-Nankai	117.16 E	39.11 N	2	1.81	0.06	0.02	0.08	-0.21	0.08	-0.09	0.05	-0.24	0.05	This study
TJ-Binhai	117.69 E	38.91 N	2	1.61	0.06	0.08	0.08	-0.26	0.06	-0.06	0.07	-0.25	0.05	
Tangshan	118.89 E	39.42 N	2	1.81	0.04	0.11	0.08	-0.22	0.07	-0.05	0.04	-0.21	0.04	
Chengde	117.77 E	41.94 N	2	1.49	0.09	0.48	0.06	-0.23	0.05	-0.06	0.05	-0.18	0.06	
Jingzhou	113.45 E	29.82 N	2	1.56	0.07	0.35	0.06	-0.20	0.09	-0.03	0.05	-0.19	0.04	
Karachi	67.13 E	24.92 N	2	5.92	0.16	-0.60	0.15	-0.04	0.11	-0.01	0.07	-0.06	0.03	
China background	-	-	15 sites	1.54	0.23	0.31	0.34	-0.15	0.06	-0.05	0.02	-0.13	0.05	(Zhang and Sun, 2026)
China urban	-	-	16 sites	3.55	1.20	-0.52	0.27	-0.05	0.04	-0.01	0.02	-0.07	0.05	
North America urban	-	-	9 sites	1.38	0.17	0.36	0.19	-0.19	0.02	-0.07	0.01	-0.17	0.03	(Tate et al., 2023)

Note: GEM concentrations (ng m^{-3}) were calculated by dividing blank-corrected Hg mass (ng) by deployment duration (days) and sampling rate (SR, m^3/day); δ202Hg values were reported after accounting for a MDF correction factor of 1.42‰. uncertainty represent the combined uncertainty calculated from the analytical uncertainty (2σ) and the standard deviation (2SD) of isotope measurements from concurrently deployed paired MerPAS units.

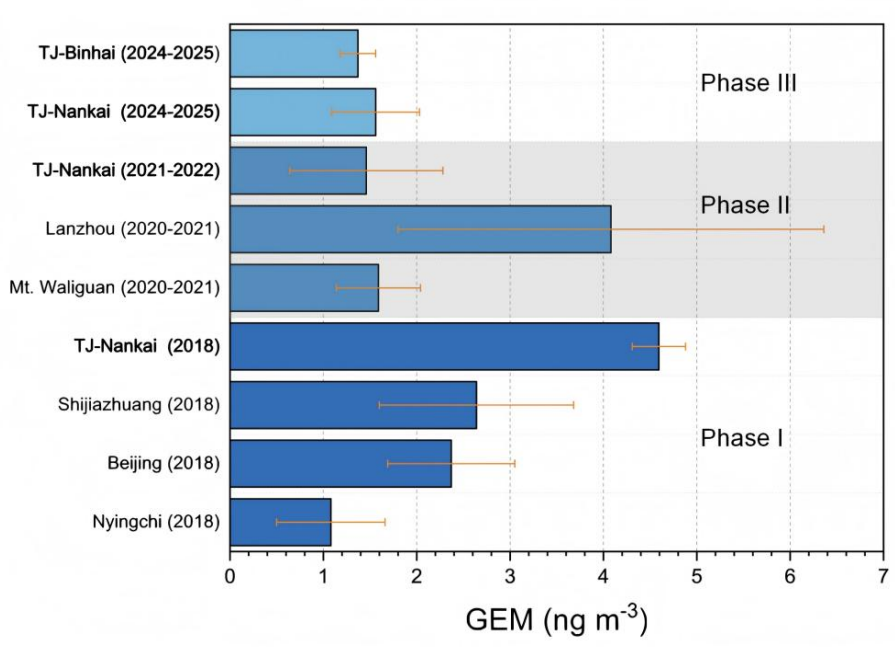

Figure S1. Comparisons of GEM concentrations between Tianjin and other sites, including Nyingchi (Yu et al., 2022), Beijing, and Shijiazhuang (Fu et al., 2021) during 2018, and Mt. Waliguan and Lanzhou (Tang et al., 2024) during 2020-2021.

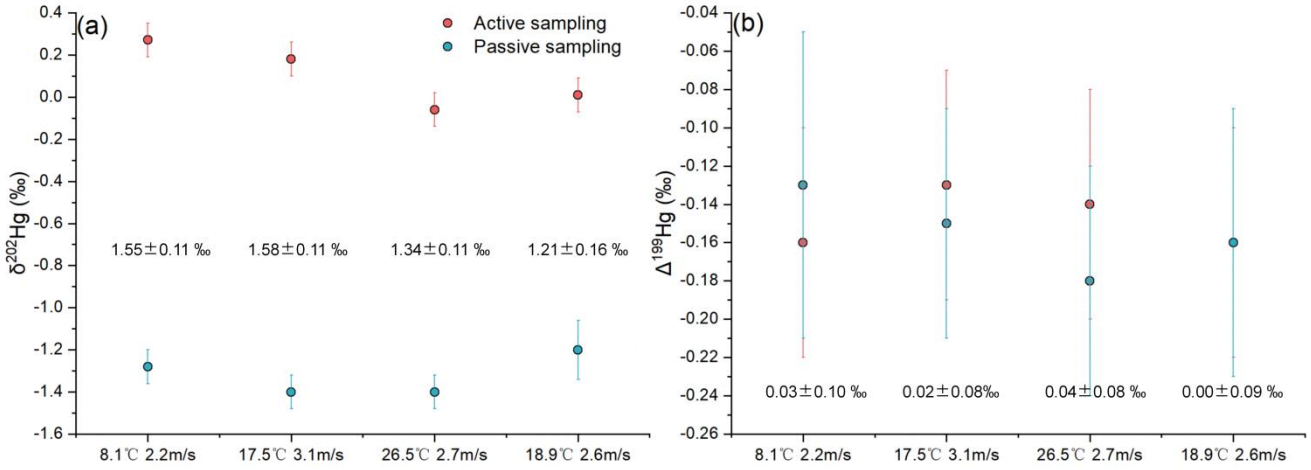

Figure S2. Results of the field calibration experiment. The calibration experiments were conducted at an outdoor site in Tianjin to evaluate the agreement of (a) δ^{202}Hg; (b) Δ^{199}Hg between samples collected by passive (MerPAS) and active samplers under varying air temperature and wind-speed conditions.

Note: Values shown represent the isotopic offset between samples collected by two sampling methods, defined as active − passive (i.e., the sample collected by the active sampler minus that collected by MerPAS). Analytic uncertainties (error bar) are method-specific: for the active sampler, uncertainty is represented by the typical 2σ analytic uncertainties of samples; for MerPAS, uncertainty is represented the combined uncertainty calculated from the analytical uncertainty (2σ) and the standard deviation (2SD) of isotope measurements from concurrently deployed paired MerPAS units.

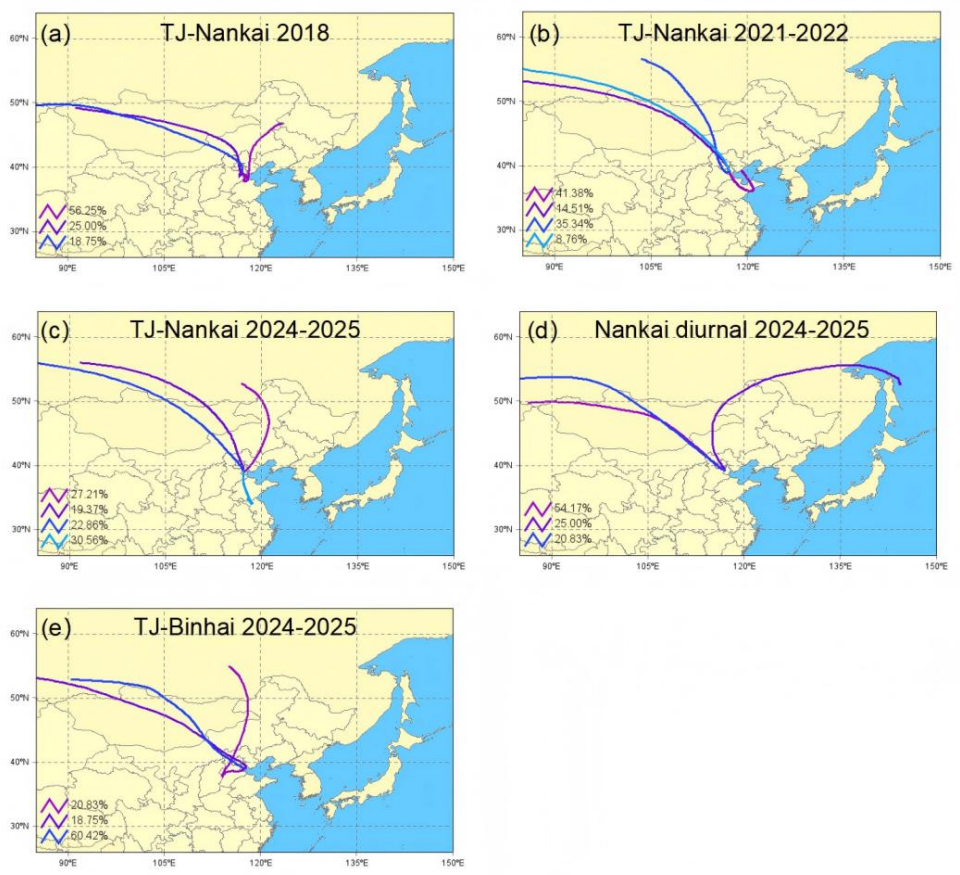

Figure S3. Air-mass backward trajectory analyses for the Nankai and Binhai sites of Tianjin city during different sampling campaigns. (a) Nankai site during November 2018, (b) Nankai site during October 2021 to September 2022, (c) Nankai stie during February 2024 to January 2025, (d) Nankai diurnal experiment during December 2024 to January 2025, and (e) Binhai site during December 2024 to January 2025. Each panel shows 120-h back trajectories arriving at 500 m above ground level during the sampling periods, calculated using the TrajStat model. Colored lines denote trajectory clusters, and the corresponding percentages represent their proportions relative to total trajectories.

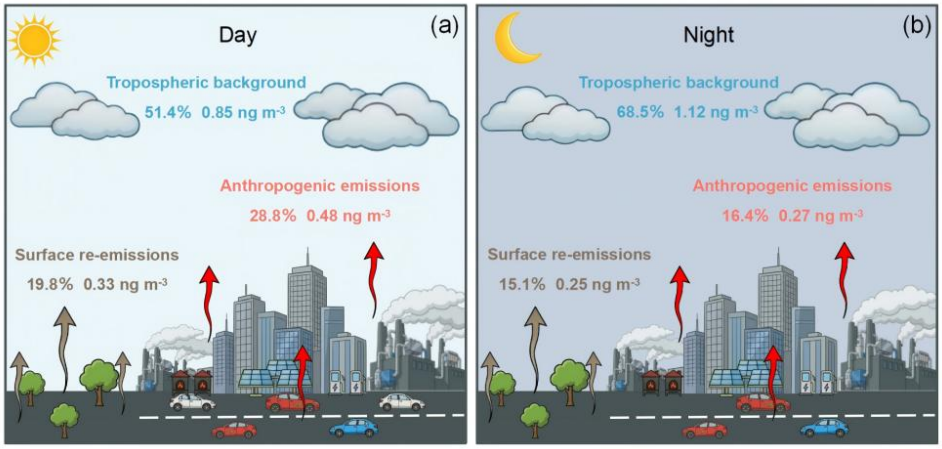

Figure S4. Source contributions to diurnal GEM concentrations in urban Tianjin during Phase III. (a) The daytime (07:00–18:00; left) and (b) nighttime (18:00–07:00; right) show the estimated relative and absolute contributions of anthropogenic emissions, surface re-emissions, and the tropospheric background to near-surface GEM concentrations.

References:

EPA-7473. *Mercury in Solids and Solutions by Thermal Decomposition*, Amalgamation, and Atomic Adsorption Spectrophotometry 1998.

EPA-1631E. *Mercury in water by oxidation, purge and trap, and cold vapor atomic fluorescence spectrometry*, EPA-821-R-02-019; Washington, DC, 2002.

Fu, X., Liu, C., Zhang, H., Xu, Y., Zhang, H., Li, J., Lyu, X., Zhang, G., Guo, H., Wang, X., Zhang, L., and Feng, X.: Isotopic compositions of atmospheric total gaseous mercury in 10 chinese cities and implications for land surface emissions, Atmos. Chem. Phys., 21, 6721–6734, https://doi.org/10.5194/acp-21-6721-2021, 2021.

Sun, R., Cao, F., Dai, S., Shan, B., Qi, C., Xu, Z., Li, P., Liu, Y., Zheng, W., and Chen, J.: Atmospheric mercury isotope shifts in response to Mercury emissions from underground coal fires, Environ. Sci. Technol., 57, 8638–8649, https://doi.org/10.1021/acs.est.2c08637, 2023.

Sun, R., Zhang, R., Yang, Y., Liu, Y., Zheng, W., Zhang, Q., Lin, H., Tong, Y., Zhang, Y., Schauer, J., Wang, X., and Chen, J.: Four decades of atmospheric mercury records at mt. Everest reveals significant reduction in anthropogenic mercury emissions over the past decade, ACS ES&T Air, 2, 824–836, https://doi.org/10.1021/acsestair.4c00296, 2025.

Szponar, N., McLagan, D. S., Kaplan, R. J., Mitchell, C. P. J., Wania, F., Steffen, A., Stupple, G. W., Monaci, F., and Bergquist, B. A.: Isotopic characterization of atmospheric gaseous elemental mercury by passive air sampling, Environ. Sci. Technol., 54, 10533–10543, https://doi.org/10.1021/acs.est.0c02251, 2020.

Tate, M. T., Janssen, S. E., Lepak, R. F., Flucke, L., and Krabbenhoft, D. P.: National-scale assessment of total gaseous mercury isotopes across the United States, J. Geophys. Res.: Atmos., 128, e2022JD038276, https://doi.org/10.1029/2022JD038276, 2023.

Tang, K., Yin, X., Zhang, H., Fu, X., Zhang, H., Zhang, L., Zhang, Q., Chen, P., Jia, L., De Foy, B., Kang, S., and Feng, X.: Transport of exogenous anthropogenic atmospheric mercury to the Tibetan Plateau identified using mercury stable isotopes, J. Geophys. Res.: Atmos., 129, e2024JD041684, https://doi.org/10.1029/2024JD041684, 2024.

Yu, B., Yang, L., Liu, H., Xiao, C., Bu, D., Zhang, Q., Fu, J., Zhang, Q., Cong, Z., Liang, Y., Hu, L., Yin, Y., Shi, J., and Jiang, G.: Tracing the transboundary transport of Mercury to the Tibetan Plateau using atmospheric mercury isotopes, Environ. Sci. Technol., 56, 1568–1577, https://doi.org/10.1021/acs.est.1c05816, 2022.

Zhang, C. and Sun, R.: Atmospheric mercury stable isotopes: advances in Mercury cycle tracing and projections of future trends, Earth Sci. Rev., 272, 105348, https://doi.org/10.1016/j.earscirev.2025.105348, 2026.